

APPARATUS AND DEMONSTRATION NOTES

Jeffrey S. Dunham, *Editor*

Department of Physics, Middlebury College, Middlebury, Vermont 05753

This department welcomes brief communications reporting new demonstrations, laboratory equipment, techniques, or materials of interest to teachers of physics. Notes on new applications of older apparatus, measurements supplementing data supplied by manufacturers, information which, while not new, is not generally known, procurement information, and news about apparatus under development may be suitable for publication in this section. Neither the *American Journal of Physics* nor the Editors assume responsibility for the correctness of the information presented. Submit materials to Jeffrey S. Dunham, *Editor*.

Simple demonstration of the central limit theorem using mass measurements

K. K. Gan, H. P. Kagan, and R. D. Kass

Department of Physics, The Ohio State University, Columbus, Ohio 43210

(Received 4 May 2000; accepted 22 March 2001)

[DOI: 10.1119/1.1379732]

Many observations from daily life and physical experiments give rise to a bell-shaped, Gaussian frequency distribution. This is a consequence of the central limit theorem (CLT) of probability. In this paper, we present a procedure for demonstrating the CLT by repeatedly measuring the mass of trays containing small steel balls. The experiment is part of a laboratory course for physics majors that emphasizes the application of statistics to data analysis.

The CLT may be stated as follows: Let Y_1, Y_2, \dots, Y_n be a sequence of n independent random variables¹ each with the same probability distribution. Suppose that the mean (μ) and variance (σ^2) of this distribution are both finite. Then the probability P for the normalized difference between the sum of the random variables and $n\mu$ to be between two numbers a and b is given by a unit Gaussian with mean at $y=0$:

$$\lim_{n \rightarrow \infty} P \left[a < \frac{Y_1 + Y_2 + \dots + Y_n - n\mu}{\sigma\sqrt{n}} < b \right] \\ = \frac{1}{\sqrt{2\pi}} \int_a^b e^{-(1/2)y^2} dy.$$

The theorem is still valid if the Y_i 's are from different probability distributions, provided each distribution has a finite mean and variance and no one term in the sum dominates. The theorem implies that under a wide range of circumstances the probability distribution that describes the sum of random variables tends toward a Gaussian distribution as the number of terms in the sum approaches infinity.

To demonstrate the CLT result that the probability distribution is consistent with a Gaussian, two experimental conditions must be satisfied:

- (i) each measurement must be the result of the sum of a large number of random variables ($n \rightarrow \infty$); and

- (ii) the number of measurements must be large to smooth out the fluctuations in the measured distribution.

It is difficult to satisfy both conditions in a classroom experiment. Fortunately, in practice a small number of random variables is adequate for the first requirement and, for the second requirement, about 30 measurements will produce a histogram that a student can recognize is Gaussian in shape. A classic demonstration of the CLT using a computer is the use of the sum of 12 random numbers to generate a Gaussian distribution. Each measurement is a sum of 12 random variables ($n=12$) with uniform probability distribution between 0 and 1. A histogram of 30 or more such measurements (sums) looks like a Gaussian frequency distribution.

For our laboratory experiment, it is convenient to write the probability for the sum to be between two numbers α and β :

$$P[\alpha < Y_1 + Y_2 + \dots + Y_n < \beta] \\ \approx \frac{1}{\sqrt{2\pi}\sigma_s} \int_{\alpha}^{\beta} e^{-(1/2)((y-\mu_s)/\sigma_s)^2} dy,$$

where $\mu_s = n\mu$ and $\sigma_s^2 = n\sigma^2$ are the mean and variance of the probability distribution for the sum. The new limits α and β are related to a and b by

$$\alpha = \mu_s + a\sigma_s, \quad \beta = \mu_s + b\sigma_s.$$

We have tested four CLT experiments in the last few years in a laboratory course for physics undergraduates in their junior year. The course also includes a computer experiment that shows that the distribution of the sum of 12 random numbers is consistent with a Gaussian; however, we believe that it is important that students perform hands-on experiments in addition to the computer simulation.

The first CLT experiment that was tried involved measuring the length of a 3 to 4 m long table using a 30 cm (1 foot)

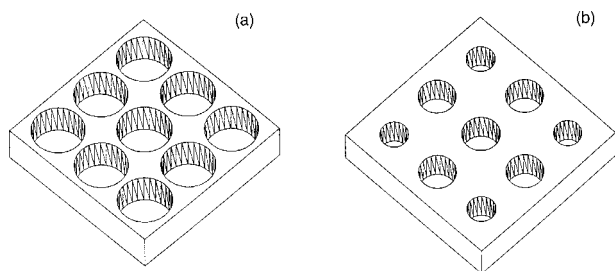


Fig. 1. Trays with nine holes of (a) same diameter (23 mm) and (b) different diameters (12 and 16 mm). The depth of the holes is 16 mm and the thickness of the trays is 19 mm.

ruler. After collecting data, a student histogrammed the table length measurements in bins of 1 cm. The measured distribution was expected to be Gaussian-like because each measurement of the table length consisted of the sum of 10 to 12 measurements with a ruler. Unfortunately, each measurement of the table length was quite tedious and time-consuming and we therefore required the student to perform a total of only 30 measurements.

The experiment was therefore replaced by a second experiment which measured the mass of 100 ml of water in a graduated 400 ml beaker. The experiment was performed using two students, A and B. Student A used two 400 ml beakers and filled one of them with water. The student carefully poured the water into the other beaker, stopping when the water level reached the 100 ml mark. After finishing the pouring, student B measured the mass of the beaker (with its 100 ml of water) using a digital scale³ with a graduation of 0.1 g. Student B did not reveal the value to student A to eliminate any potential bias. Student A then emptied the beaker, dried it off with a paper towel and repeated the process a total of 30 times. The students then switched roles so that a second set of measurements is obtained for student B. The students histogrammed the mass measurements in bins of 0.5 g. In this experiment, there were two sources of uncertainties. First, it was impossible to control the exact amount of water poured, resulting in under or over pour. Second, it was difficult to tell if the water level was exactly at the 100 ml mark due to the capillary effect. These two (desirable, for the purposes of this experiment) effects yielded a Gaussian-like distribution for the measured mass. This experiment was less tedious than the first experiment but was still too time-consuming. To save time, we required the students to perform only 30 measurements. However, the problem with an experiment with only 30 measurements is that some students will see large fluctuations, resulting in a distribution that does not look like a Gaussian although the distribution is statistically consistent with a Gaussian. For the untrained eyes of a student, this is not good evidence for the CLT. An experiment that allows the collection of approximately 100 measurements in a reasonable amount of time would give a better demonstration of the theorem.

We therefore tried a third experiment, involving measurement of the mass of cans containing very small steel balls.⁴ Each ball had a diameter of 3.2 mm and mass of 0.13 g. We used as a can the plastic container that typically comes with 35 mm film. This had a diameter of 3 cm and height of 5 cm. A student filled a small plastic beaker with balls and then poured the balls into a can. The student then used a wood stick to wipe across the top of the can to remove excess balls. The student should always wipe in the same manner to en-

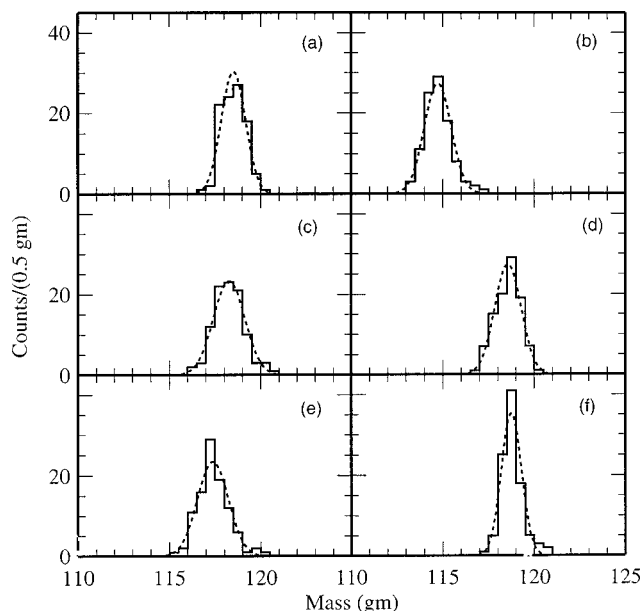


Fig. 2. The mass distributions of trays containing steel balls as measured by six students using the tray of Fig. 1(b). The dashed curves show the result of a Gaussian fit.

sure that approximately the same number of balls remain in the can. All the manipulations were done above a large container to prevent the loss of balls. The process was repeated a total of 100 times, which took a total of about 30 min. The student then histogrammed the mass measurements in bins of 0.5 g. In this experiment, there were two contributions to the uncertainty in the number of balls in each can (and hence the total mass). One was the packing of the balls which was slightly different for each pouring. The other was the slightly different number of balls being removed by each wipe. Due to the two uncertainties, a slightly different mass was obtained each time. The measured mass distribution looked Gaussian.

It is difficult to explain the observed Gaussian distribution using the CLT because we do not know the number of random variables (n) in the experiment. We have therefore modified the experiment to measure the total mass of the steel balls in a tray which contains nine small holes ($n=9$) as shown in Fig. 1(a), with the mass of balls in each hole representing a random variable. The tray is made of a sturdy but machinable foam.⁵ The procedure for this experiment is similar to the previous experiments; however, it takes a

Table I. χ^2 per degree of freedom (DOF) and confidence level (CL) for a Gaussian distribution fitted to the mass distributions shown in Figs. 2 and 3.

Figure	χ^2/DOF	CL (%)
2(a)	5.3/5	39
2(b)	5.9/6	44
2(c)	5.3/8	72
2(d)	2.3/5	81
2(e)	8.8/7	27
2(f)	8.3/4	8
3(a)	45/9	0.0001
3(b)	33/13	0.2

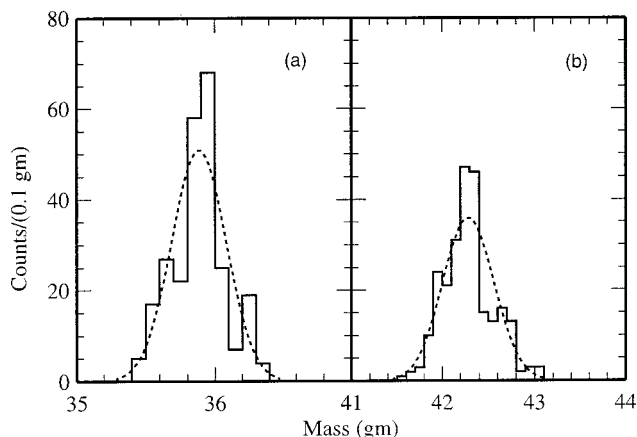


Fig. 3. The mass distributions of the steel balls in the small (a) and big (b) holes in the tray of Fig. 1(b). The dashed curves show the result of a Gaussian fit.

longer time (1 h) to accumulate 100 data points. The measured mass distribution looks Gaussian, as expected from the CLT.

We can also modify this experiment to illustrate the CLT when the random variables have different probability distributions. Thus we have another version of the experiment in which the tray has holes of two different diameters (four of 12 mm and five of 16 mm) as shown in Fig. 1(b). The results from six students are shown in Fig. 2. The means of the distributions are slightly different for each student because

students wipe the excess balls off differently. Each distribution is fitted to a Gaussian and the χ^2 per degree of freedom and confidence level are summarized in Table I. It is evident that the distributions are consistent with a Gaussian distribution and the statistics are quite adequate. To verify that the Gaussian distribution is not the result of the sum of nine Gaussian distributions,⁶ we measure the mass distributions of the balls in the individual holes of different diameters and the results are shown in Fig. 3. The distributions have a more pronounced peak and fit poorly to a Gaussian distribution as evident from the large χ^2 per degree of freedom and low confidence level given in Table I.

In summary, we have a simple procedure for demonstrating the central limit theorem in an acceptable length of time for a laboratory experiment.

The authors wish to thank Alan Van Heuvelen for advice and encouragement, Mike Gee for the countless measurements of the mass distributions, and the Machine Shop of the Department of Physics for the excellent machining job.

¹A random variable is any function that associates a number with each possible outcome. See, for example, J. L. Devore, *Probability and Statistics for Engineering and the Sciences* (Brooks/Cole, Pacific Grove, CA, 1991), 3rd ed., pp. 80–83.

²See, for example, G. Cowan, *Statistical Data Analysis* (Oxford U. P., Oxford, 1998), pp. 147–149.

³Acculab digital scale, model V-333.

⁴The steel balls were purchased from McMaster-Carr.

⁵Last-A-Foam FR6725, General Plastics Mfg. Co.

⁶The contribution to the width of the Gaussian from the spread in the mass of the balls is small since the ball mass is measured to be uniform to within 0.3% (standard deviation).

Magnetically driven chaotic pendulum

John P. Berdahl and Karel Vander Lugt^{a)}

Department of Physics, Augustana College, Sioux Falls, South Dakota 57197

(Received 15 July 1999; accepted 24 April 2001)

[DOI: 10.1119/1.1387041]

I. INTRODUCTION

A recent article in this journal compared several commercial chaotic pendulum systems.¹ The data obtained are impressive, but the units are rather expensive. This project describes a simple, robust, and inexpensive way to demonstrate and analyze chaotic motion quantitatively in the lab. We use a relatively inexpensive physical pendulum in conjunction with typical data acquisition equipment (rotary motion sensor, photogate, and computer). The pendulum is driven by a rotating permanent magnet. The data are analyzed by plotting them in phase space, looking at time-delay plots, finding the Poincaré section, and taking the Fourier transform. Examples of both periodic and chaotic motion are illustrated.

II. EQUIPMENT

The physical pendulum was purchased from Team Labs² and is shown in Fig. 1 attached to a rotary motion probe. It can be described as a “triple” pendulum. The three longer arms, fixed at 120° from each other, are 12 cm long, and each

has a 10-cm-long pendulum attached to it with a precision roller bearing. Each of the three pendulums has a 40-g disk that can be adjusted along the length of the pendulum to change its natural frequency. The mass of the complete apparatus is 470 g. It has four degrees of freedom and oscillates, at least visually, in a complex and seemingly haphazard manner. To enable the pendulum to be driven, a permanent magnet is attached to its front. Two rectangular (1 × 0.5 × 0.125 in.) rare earth magnets purchased from Edmund Scientific³ were placed adjacent to each other and taped to the pendulum. The body of the pendulum is attached to the rotary motion probe, which reads the angle of displacement forty times per second with a resolution of 0.25°. To keep the angular displacement between $-\pi$ and $+\pi$ rad, the point of attachment of the pendulum to the rotary probe was offset 2 cm from the geometrical center. The data acquisition system sends the measurements directly to a spreadsheet. Typically, 12 000 data points are acquired for each run.

To drive the pendulum, a rotating permanent magnet is placed 1–2 cm in front of the magnets attached to the pen-

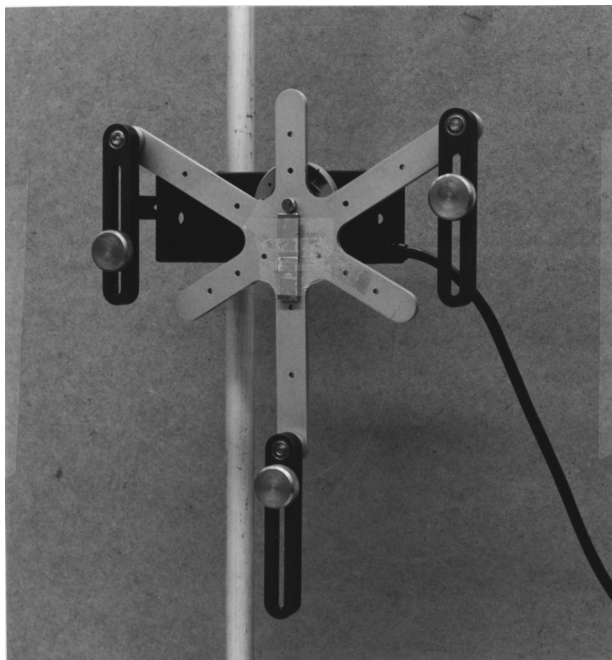


Fig. 1. The “triple” pendulum used in this project attached to a rotary motion probe. Both are mounted on a vertical support rod.

dulum, as shown in Fig. 2. We used a cattle rumen magnet measuring $6.5 \times 2.0 \times 0.8$ cm, but any long rare earth magnet will work equally well. The driving magnet can be rotated with any variable, low-speed, high-torque motor.

The rotation speed of the driving magnet is the only parameter that is varied from run to run; everything else is left the same. Different rotation speeds result in different long-term behavior of the “triple” pendulum. At some driving frequencies, the pendulum motion is periodic (period-one,

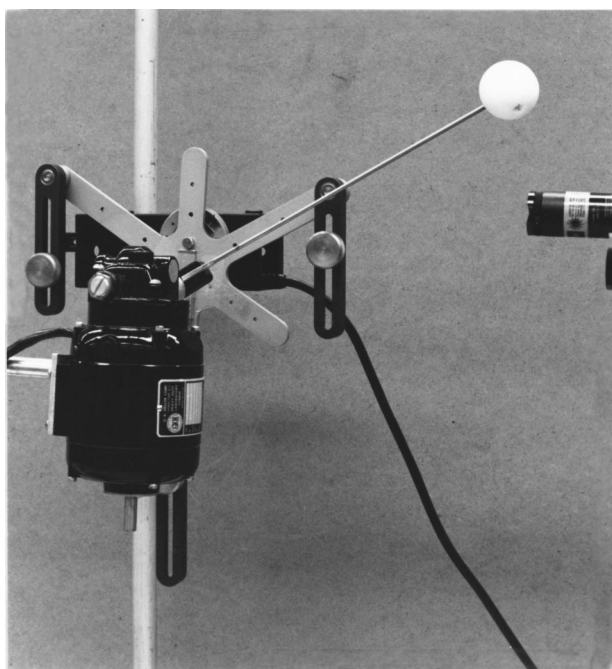


Fig. 2. Experimental arrangement for driving the pendulum and for determining the phase of the driving force. The small ball on the thin rod intercepts the photogate once each rotation of the driving magnet.

period-two, period-three, etc.) while for others it is chaotic. To estimate the amount of damping, we observed that when not driven, i.e., when swinging naturally, the pendulum takes 50 s (about 30 oscillations) for the amplitude to fall to $1/e$ of its initial value.

It is easy to plot the path of the pendulum in phase space by plotting angular displacement, θ in radians, against angular velocity, Ω in radians per second. Angular velocity was calculated by taking the difference between adjacent angular position readings and then averaging over three adjacent velocity values to smooth it. We also wanted to observe Poincaré sections. In order to “strobe” the pendulum’s path in phase space once each rotation of the driving magnet, the displacement angle of the pendulum must be determined at a particular phase of the driving magnet. A rod was attached to the shaft of the motor and a standard photogate was used to determine the phase of the driving magnet. Each time a small styrofoam ball attached to the rod intercepted the photogate’s light beam, the event was recorded. Figure 2 shows the arrangement. In this way one is able to “strobe” the path of the pendulum in phase space. The Poincaré section is obtained by plotting only those points in phase space that are simultaneous (within 0.025 s in our case) with the photogate events. An additional benefit of using the photogate is that the effect of feedback from the pendulum to the motor can be monitored. Since the timing between photogate events was very consistent in all cases, we conclude that coupling between the pendulum and motor was not a complicating factor.

III. RESULTS

In this project, the data acquisition system places the data directly into a spreadsheet. The analysis and graphing could be done from within the spreadsheet, but we transferred the data into a more flexible program called MATLAB, where all graphing and analysis was done.

Figure 3(a) shows the displacement angle, θ , of the pendulum as a function of time for a short segment of a 300-s run. The driving magnet was rotated at a frequency of 3.33 Hz. To avoid transients we waited at least 5 min after the driving magnet was turned on before recording data. The periodic steady-state behavior of the pendulum is evident in Fig. 3(a).

The power spectrum (absolute value of the Fourier transform) of the data is shown in Fig. 3(b). The resolution in the frequency domain is obtained by dividing the sampling rate by the length of the data array. For the data of Fig. 3(b) the frequency resolution is 0.0033 Hz, which is the spacing between points along the frequency axis. There is a small peak at the driving frequency of 3.33 Hz, and another small peak at 2.22 Hz, but by far the largest component is a subharmonic at 1.11 Hz. In particular, the power spectrum consists of a small set of discrete harmonic frequencies. This characteristic was observed in all cases of periodic motion.

The path of the motion in phase space (Ω vs θ) is shown in Fig. 4(a). Essentially, it is an oval with two small kinks in it. (The width of the oval is a result of being limited to a sampling rate of only forty samples per second.)

When studying chaotic motion the Poincaré section is of considerable interest. It is obtained by strobing the path in phase space once per driving cycle. The Poincaré section in

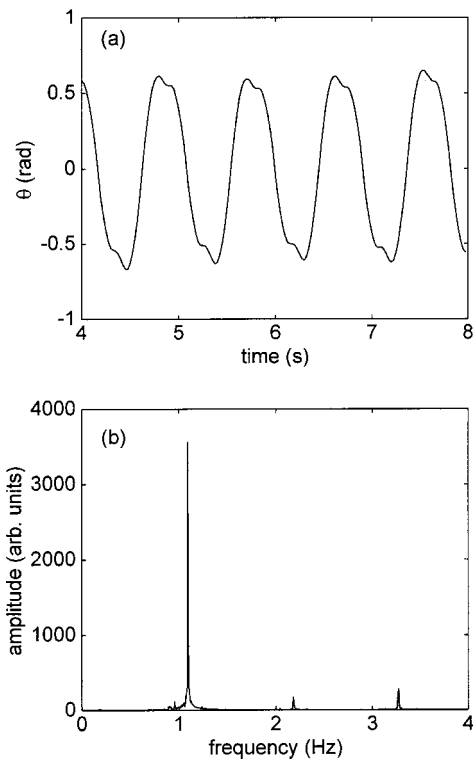


Fig. 3. (a) A typical segment of data showing the angle of the pendulum as a function of time. The driving frequency of the rotating magnet is 3.33 Hz. The motion is periodic. (b) The power spectrum of 12 000 data points showing only three discrete, harmonically related frequencies.

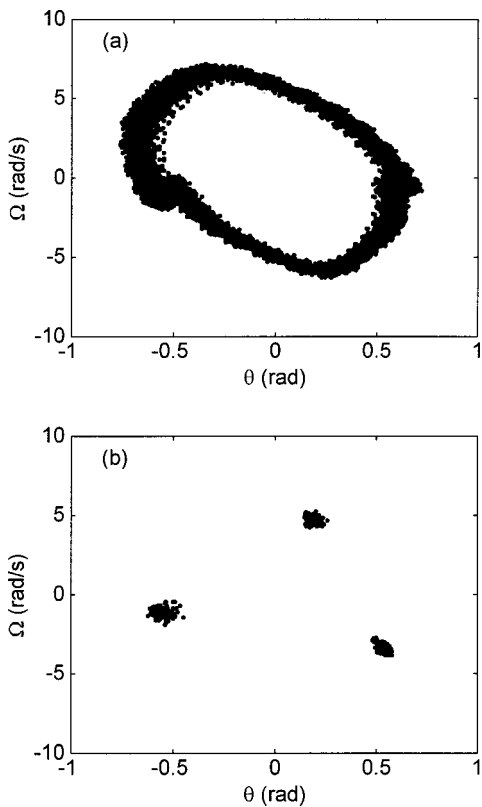


Fig. 4. (a) The path in phase space (displacement angle vs angular velocity) for the data of Fig. 3. (b) The Poincaré section showing that the long-term behavior is a period-three orbit.

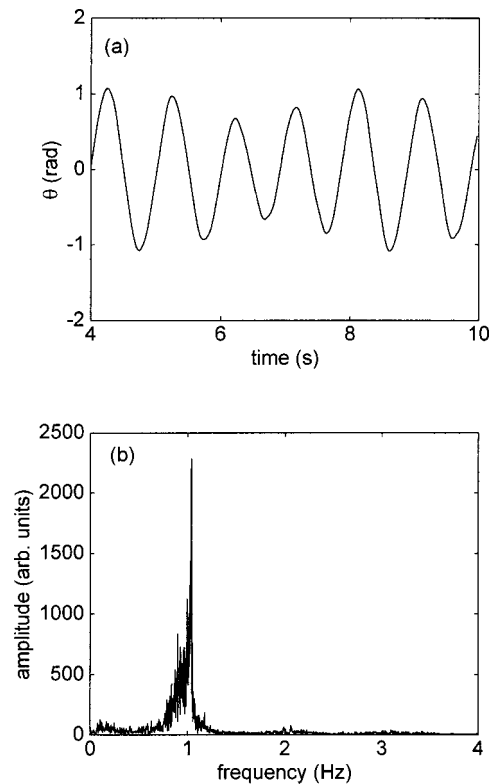


Fig. 5. (a) A typical segment of data showing the angle of the pendulum as a function of time for a driving frequency of 2.106 Hz. The motion does not appear to repeat. (b) The power spectrum showing a continuum of frequencies, rather than discrete, harmonically related frequencies.

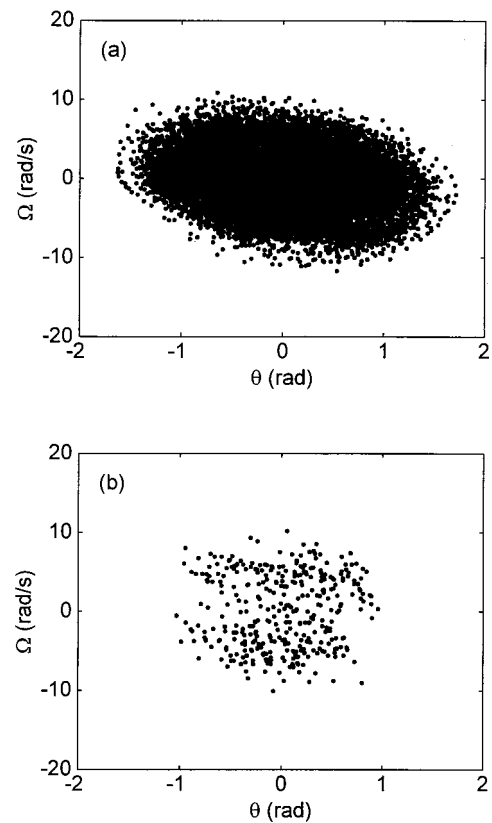


Fig. 6. (a) The path in phase space for the data of Fig. 5. The maximum angle is approximately 1.7 rad. (b) The Poincaré section shows that the long-term behavior is not periodic, but chaotic. This conclusion is consistent with the power spectrum of Fig. 5(b).

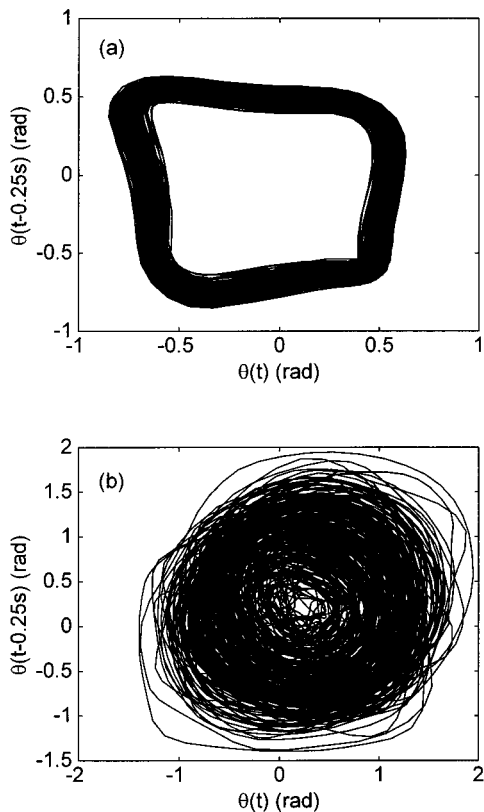


Fig. 7. (a) A time-lag plot for the case of periodic motion. (b) A time-lag plot for the case of chaotic motion. In both plots the time lag is 0.25 s or 10 data points.

Fig. 4(b) shows that the steady-state motion in this case is a period-three orbit, i.e., the driving magnet rotates three times for each swing of the pendulum.

At some driving frequencies, Poincaré sections with dis-

crete spots (periodic orbits) are observed while at other frequencies the motion is chaotic. Figure 5(a) shows the displacement angle of the pendulum versus time for a driving frequency of 2.106 Hz. The power spectrum, Fig. 5(b), in this case is not a set of discrete harmonic frequencies, but is spread out over a continuous range of frequencies. The maximum amplitude in the frequency spectrum occurs at 1.036 Hz, which is roughly half the driving frequency.

The path in phase space is seen in Fig. 6(a). It essentially fills the oval area and suggests that the pendulum does not repeat any set pattern. The Poincaré section is shown in Fig. 6(b) and does not consist of a small number of discrete spots; rather, it is a complex subset of phase space. Theoretically, one expects that it is a strange attractor with fractal geometry. To explore the details of the strange attractor experimentally, one would need a data acquisition system with a higher sampling rate and collect much more data. In addition to looking at the Poincaré section, we also observed time-lag plots. The value of the displacement angle at time t , $\theta(t)$, is plotted against the value of the displacement angle a short time Δt earlier, $\theta(t - \Delta t)$. We viewed time lags from 0.025 to 1 s, that is, from one to forty data points apart. A time-lag plot for periodic motion is shown in Fig. 7(a) while a time-lag plot for chaotic motion is shown in Fig. 7(b). In both cases the time lag was 10 data points or 0.25 s. In the case of periodic motion, the time-lag plot is a closed, distinct loop. In the case of chaotic motion, any underlying structure that may exist remains hidden. More accurate data and more data points would be needed to reveal structure in either the Poincaré sections or the time-lag plots in the chaotic motion cases.

^aElectronic mail: vanderlu@inst.augie.edu

¹James A. Blackburn and Gregory L. Baker, "A comparison of commercial chaotic pendulums," *Am. J. Phys.* **66** (9), 821–830 (1998).

²Team Labs, 6859 North Foothills Hwy., Boulder, CO 80302.

³Edmund Scientific Company, 101 East Gloucester Pike, Barrington, NJ 08007.